REPORT DOCUMENTATION PAGE

Form Approved
OMB No. 0704-0188

1. REPORT DATE *(DD-MM-YYYY)*	2. REPORT TYPE	3. DATES COVERED *(From - To)*
	Technical Papers	

4. TITLE AND SUBTITLE

Please see attached

5a. CONTRACT NUMBER

5b. GRANT NUMBER

5c. PROGRAM ELEMENT NUMBER

6. AUTHOR(S)

5d. PROJECT NUMBER
4847

5e. TASK NUMBER
0052

5f. WORK UNIT NUMBER
549927

7. PERFORMING ORGANIZATION NAME(S) AND ADDRESS(ES)

Air Force Research Laboratory (AFMC)
AFRL/PRS
5 Pollux Drive
Edwards AFB CA 93524-7048

8. PERFORMING ORGANIZATION REPORT

9. SPONSORING / MONITORING AGENCY NAME(S) AND ADDRESS(ES)

Air Force Research Laboratory (AFMC)
AFRL/PRS
5 Pollux Drive
Edwards AFB CA 93524-7048

10. SPONSOR/MONITOR'S ACRONYM(S)

11. SPONSOR/MONITOR'S NUMBER(S)
Please see attached

12. DISTRIBUTION / AVAILABILITY STATEMENT

Approved for public release; distribution unlimited.

13. SUPPLEMENTARY NOTES

14. ABSTRACT

20030205 171

15. SUBJECT TERMS

16. SECURITY CLASSIFICATION OF:			17. LIMITATION OF ABSTRACT	18. NUMBER OF PAGES	19a. NAME OF RESPONSIBLE PERSON
					Leilani Richardson
a. REPORT	b. ABSTRACT	c. THIS PAGE	A		19b. TELEPHONE NUMBER *(include area code)*
Unclassified	Unclassified	Unclassified			(661) 275-5015

[redacted]

DTS ✓

48470052

MEMORANDUM FOR PRS (In-House Publication)

FROM: PROI (TI) (STINFO) 03 Jan 2001

SUBJECT: Authorization for Release of Technical Information, Control Number: **AFRL-PR-ED-TP-2001-002**
Fife, J.M., "The Effects of Insulator Wall Material on Hall Thruster Discharges: A Numerical Study"

AIAA Technical Conference - Aerospace Sciences Conferences **(Statement A)**
(Reno, NV, 10 Jan 2001) **(Deadline: 05 Jan 2001)**

The Effects of Insulator Wall Material on Hall Thruster Discharges: A Numerical Study

John Michael Fife
Air Force Research Laboratory
Edwards AFB. California

Summer Locke
University of Washington
Seattle. Washington

An investigation was undertaken to determine how the choice of insulator wall material inside a Hall thruster discharge channel might affect thruster operation. In order to study this. an evolved hybrid particle-in-cell (PIC) numerical Hall thruster model. HPHall. was used. HPHall solves a set of quasi-one-dimensional fluid equations for electrons. and tracks heavy particles using a PIC method. The two systems are linked by charge neutrality. Five cases were executed with various secondary electron emission coefficients at the insulator wall. Results show a steady increase in thruster efficiency from 0.434 to 0.483 as secondary electron emission coefficient is decreased by 2/3. This suggests that secondary electron emission be one of the parameters considered during the Hall thruster design phase, and that channel insulator materials with low secondary electron emission should be favored.

Introduction

The choice of ceramic insulator material for Hall thruster discharge chambers is largely dependent on structural and thermal requirements. as well as resistance to ion sputtering. Analysis has recently indicated that the secondary electron emission coefficient of the discharge channel insulator may affect the plasma discharge and. therefore. also be an important Hall thruster design parameter. This paper investigates changes in the Hall thruster discharge for various secondary electron emission coefficients using a numerical Hall thruster simulation, *HPHall*.

Several numerical simulations of Hall thrusters have been developed by other reseachers.[1,2] *HPHall* is a two-dimensional transient hybrid particle-in-cell (hybrid PIC) simulation. Although descriptions of *HPHall* have been presented before,[3-6] a brief summary of the model and method will be repeated here.

Governing Equations

Although this transient 2-D 3-V simulation operates in cylindrical coordinates (z, r, v_z, v_r, v_θ), some vector quantities in the analysis below are written with respect to the magnetic field lines. As Fig. 1 shows. $\hat{n}$ and $\hat{t}$ are used to represent the distance vectors normal and tangent to the magnetic field lines. respectively.

Electrons

The simplified electron equations consist of a generalized Ohm's law, a current conservation equation, and an electron temperature equation. Assuming a Maxwellian electron distribution. quasineutrality, and a particular ion field, these three equations are sufficient to yield electron current density. space potential, and electron temperature as a function of time.

The diffusion coefficient of electrons along magnetic field lines is assumed to be much greater than the diffusion coefficient across them. Ignoring the magnetic mirror effect, and assuming constant electron temperature along magnetic field lines, the momentum equation gives,

$$\phi + \frac{kT_e}{e}\ln(n_e) = \phi^*(\lambda) . \qquad (1)$$

Note that Eq. (1) holds along magnetic field lines. λ is a magnetic stream function which is constant for any given field line.

Electron diffusion across the magnetic field is assumed to obey a Generalized Ohm's Law. In the lab frame, the cross-field electron velocity in terms of an effective electron mobility across the magnetic field lines, $\mu_{e\perp}$, is

$$u_{e\hat{n}} = -\mu_{e\perp}\left(E_{\hat{n}} + \frac{1}{en_e}\frac{\partial p_e}{\partial \hat{n}}\right). \qquad (2)$$

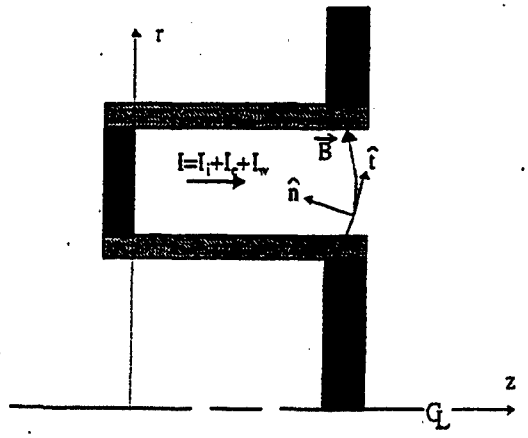

Fig. 1. Diagram showing a simplified Hall thruster discharge channel cross section, the coordinate system used, and the current convention.

Classical cross-field mobility in the weakly ionized limit[7] ($\sim 1/B^2$) has been shown[8] not to adequately describe the high electron transport across lines of force in the presence of a strong magnetic field. Some previous work has suggested that the discrepancy between measured and predicted mobility may be due to anomalous "Bohm" diffusion,[9] which goes as $1/B$. Neither classical nor Bohm models appropriately describe the mobility throughout the discharge channel. It is believed that, in some regions, other mechanisms, such as wall conductivity or wave transport, may dominate. However, in the interest of exploring the physics of the acceleration process, we use classical and Bohm mobility here.

$$\mu_{e\perp} = \frac{\mu_e}{\beta_e^2} + K_B \frac{1}{16B}, \qquad (3)$$

and leave the coefficient, K_B, as an adjustable parameter between 0 and 1. Based on comparison with experimental data, the "best" K_B was found to be .15.

Current Conservation

Since quasineutrality is imposed, no space charge can accumulate, and current must be conserved for the whole device. A conservation equation for current crossing any magnetic field line can be written $I_o = I_e + I_i + I_w$, where I_o, I_e, I_i, and I_w are the discharge, electron, ion, and near-wall currents, respectively. In terms of integrals along magnetic field lines,

$$I_o = -2\pi e \int_0^l n_e u_{e,s} r ds + 2\pi e \int_0^l n_e u_{i,s} r ds + I_w. \qquad (4)$$

By combining Eqs. (1) through (4) a differential equation may be obtained for the cross-field variation of ϕ^*.

Electron Energy Equation

An electron energy equation is derived under the assumptions that electrons have a Maxwellian velocity distribution, and that the pressure dyad reduces to a scalar pressure term, $n_e k T_e$. Source terms include losses due to ionization, radiation, and charge-field interactions. Ionization and radiation losses are modeled analytically with a net ion production cost according to Dugan and Sovie.[10] Charge-field interactions are modeled as j_e^2/σ_e. The energy equation is applied across magnetic field lines only. Along them, electrons are assumed to be isothermal.

Ionization Rate

The bulk electron-neutral ionization rate is determined by integrating the Drawin[7] cross-section over a Maxwellian electron distribution. This bulk ionization rate, plus the equations of motion for the ions and neutrals, completes the model for those species.

Modeling Wall Effects

Interaction of the Hall thruster plasma with the insulator wall depends upon secondary electron emission coefficient of the wall material. Previous models[3] assumed zero or constant secondary electron emission coefficient, resulting in very low electron energy flux to the wall. This caused high predictions of T_e. The following theory is a more detailed approach, parts of which have been published before.[5,6,11] Also, Katz et al.[12] present an analogous theory for computation of charging rate on geosynchronous spacecraft.

Experimental data show that the ratio of secondary to primary electrons, δ, is a function of incident electron energy, E (eV). At low (<100eV) energies, an exponential fit can be used to closely approximate $\delta(E)$:

$$\delta = AE^B \qquad (5)$$

First we look at a negative wall potential with respect to the plasma ($\phi_w < 0$), and an ion-attracting sheath. From sheath theory, the primary electron flux is,

$$\Gamma_e = \frac{n_e \bar{c}_e}{4}, \qquad (6)$$

where $\bar{c}_e$ is the electron mean thermal speed. The integral,

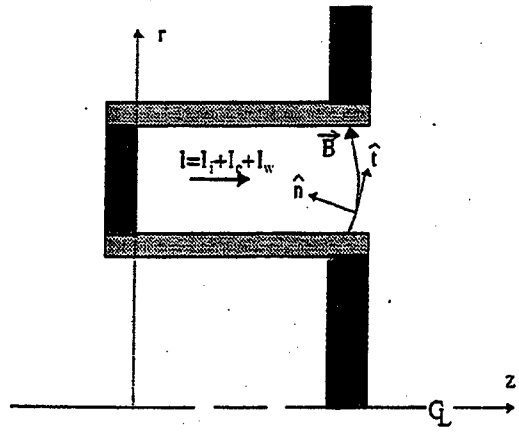

Fig. 1. Diagram showing a simplified Hall thruster discharge channel cross section, the coordinate system used, and the current convention.

Classical cross-field mobility in the weakly ionized limit[7] ($\sim 1/B^2$) has been shown[8] not to adequately describe the high electron transport across lines of force in the presence of a strong magnetic field. Some previous work has suggested that the discrepancy between measured and predicted mobility may be due to anomalous "Bohm" diffusion,[9] which goes as $1/B$. Neither classical nor Bohm models appropriately describe the mobility throughout the discharge channel. It is believed that, in some regions, other mechanisms, such as wall conductivity or wave transport, may dominate. However, in the interest of exploring the physics of the acceleration process, we use classical and Bohm mobility here.

$$\mu_{e\perp} = \frac{\mu_c}{\beta_c^2} + K_B \frac{1}{16B}. \qquad (3)$$

and leave the coefficient, K_B, as an adjustable parameter between 0 and 1. Based on comparison with experimental data, the "best" K_B was found to be 0.15.

Current Conservation

Since quasineutrality is imposed, no space charge can accumulate, and current must be conserved for the whole device. A conservation equation for current crossing any magnetic field line can be written $I_d = I_e + I_i + I_w$, where I_d, I_e, I_i, and I_w are the discharge, electron, ion, and near-wall currents, respectively. In terms of integrals along magnetic field lines,

$$I_d = -2\pi e \int_0^l n_e u_{e,B} r ds + 2\pi e \int_0^l n_e u_{i,B} r ds + I_w. \qquad (4)$$

By combining Eqs. (1) through (4) a differential equation may be obtained for the cross-field variation of ϕ^*.

Electron Energy Equation

An electron energy equation is derived under the assumptions that electrons have a Maxwellian velocity distribution, and that the pressure dyad reduces to a scalar pressure term, $n_e k T_e$. Source terms include losses due to ionization, radiation, and charge-field interactions. Ionization and radiation losses are modeled analytically with a net ion production cost according to Dugan and Sovie.[10] Charge-field interactions are modeled as j_e^2/σ_e. The energy equation is applied across magnetic field lines only. Along them, electrons are assumed to be isothermal.

Ionization Rate

The bulk electron-neutral ionization rate is determined by integrating the Drawin[7] cross-section over a Maxwellian electron distribution. This bulk ionization rate, plus the equations of motion for the ions and neutrals, completes the model for those species.

Modeling Wall Effects

Interaction of the Hall thruster plasma with the insulator wall depends upon secondary electron emission coefficient of the wall material. Previous models[3] assumed zero or constant secondary electron emission coefficient, resulting in very low electron energy flux to the wall. This caused high predictions of T_e. The following theory is a more detailed approach, parts of which have been published before.[5,6,11] Also, Katz et al.[12] present an analogous theory for computation of charging rate on geosynchronous spacecraft.

Experimental data show that the ratio of secondary to primary electrons, δ, is a function of incident electron energy, E (eV). At low (<100eV) energies, an exponential fit can be used to closely approximate $\delta(E)$:

$$\delta \approx AE^B \qquad (5)$$

First we look at a negative wall potential with respect to the plasma ($\phi_w < 0$), and an ion-attracting sheath. From sheath theory, the primary electron flux is,

$$\Gamma_e = \frac{n_e \bar{c}_e}{4}, \qquad (6)$$

where $\bar{c}_e$ is the electron mean thermal speed. The integral,

$$\Gamma_{sec} = \int w_\perp f_e(w)\delta d^3w . \qquad (7)$$

yields the secondary electron flux, $\Gamma_{sec} = \Gamma_e\delta_{eff}$, and the effective secondary emission coefficient, δ_{eff}, in the form:

$$\delta_{eff} = \Gamma[2+B]A(kT_e/e)^B . \qquad (8)$$

where $\Gamma[x]$ is Euler's Gamma function.

Imposing wall neutrality by balancing the fluxes of ions and primary and secondary electrons, it can be shown that,

$$\phi_w = \frac{-kT_e}{e}\ln[(1-\delta_{eff})e^{1/2}\frac{\bar{c}_e}{4v_b}], \qquad (9)$$

where the Bohm velocity is,

$$v_b = \sqrt{\frac{kT_e}{m_i}} . \qquad (10)$$

From (9), the sheath potential reverses at a breakpoint temperature, $T_{e.BP}$, where,

$$[(1-\delta_{eff})e^{1/2}\frac{\bar{c}_e}{4v_b}] = 1 . \qquad (11)$$

The wall potential is negative for $T_e < T_{e.BP}$, and positive for $T_e > T_{e.BP}$. For xenon and boron nitride (a candidate insulator for Hall thrusters, for which $A = 0.141$ and $B = 0.576$),[13] $T_{e.BP} = 16.55eV$, and $\delta_{eff} = 0.997$.

For the case of the ion-repelling sheath, the neutrality condition requires that $\delta_{eff} \approx 1$. Since secondaries must now overcome the sheath barrier to escape into the plasma, the (slightly positive) wall potential is:

$$\phi_w = \frac{kT_{sec}}{e}\ln[\Gamma[2+B]A(kT_e/e)^B] . \qquad (12)$$

This is of the order T_{sec}, which is the temperature of the secondary electrons, no more than $\sim 1eV$.

An equation for electron energy lost to the wall and sheath is obtained by integrating the primary and secondary electron energy fluxes across Maxwellian distributions:

$$q_{wall} = \int w_\perp f_e(w)(\tfrac{1}{2}m_e w^2)d^3w - \int w'_\perp f_e(w')(\tfrac{1}{2}m_e w^2)d^3w' \qquad (13)$$

where $w_\perp$ is the primary electron velocity component normal to the wall and where $w'_\perp$ is the velocity of the secondary electrons assumed to be Maxwellian at temperature T_{sec}. The integral yields:

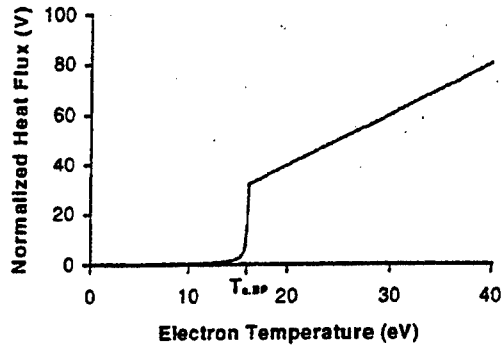

Fig. 2. Normalized heat flux to the wall versus electron temperature for xenon on boron nitride.

$$q_{wall} = \Gamma_e[2kT_e - e\phi_w] - \Gamma_e\delta_{eff}[2kT_{sec} - e\phi_w] . \qquad (14)$$

Thus, for $T_e < T_{e.BP}$ and $T_e > T_{e.BP}$, respectively:

$$\frac{q_{wall}}{j_e} = \frac{1}{e}\exp\frac{e\phi_w}{kT_e}[2k(T_e - \delta_{eff}T_{sec}) - (1-\delta_{eff})\phi_w] ; \qquad (15)$$

$$\frac{q_{wall}}{j_e} = \frac{1}{e}[2k(T_e - T_{sec})] , \qquad (16)$$

where $j_e = en_e\bar{c}_e/4$. A graph of this is shown in Fig. 2. Notice the sharp increase in heat loss to the wall around $T_{e.BP}$. In fact, the heat loss grows so large at $T_{e.BP}$ that it effectively limits the electron temperature to $T_{e.BP}$.

Sheath and secondary emission effects are also important when considering cross-field electron transport near the wall. The low-energy secondary electrons are assumed to start from rest at the wall in crossed electric and magnetic fields. By calculating the distance traveled downstream by their guiding centers, an expression for the total near-wall electron conductivity is determined:

$$l_w = e\delta_{eff}\left(\frac{2\pi Em_e}{B^2\sin(\theta)}\right). \qquad (17)$$

Above, δ_{eff} is the effective secondary emission yield, and θ is the angle of incidence of the magnetic field line with the wall.

Boundary Conditions

The boundary conditions for the quasi-1-D electron equations are handled by directly fixing T_e at the

cathode, and by imposing a zero-slope condition on T_e at the anode.

HPHall is capable of modeling background (chamber) pressure at the downstream boundary[13,14] however, the background pressure is set to zero for this study. The boundary conditions at the injector also include the introduction of particles from the propellant feed. These particles are placed randomly within the injector region, and take random trajectories corresponding to a half-range Maxwellian at a temperature of 1000 degK.

Numerical Method

The governing equations are solved time-accurately by separating the slow time scale (ion and neutral) motion from the fast time scale (electron) motion, and iterating successively. Individual ion and neutral atoms are simulated using a Particle-In-Cell method. The electron motion is modeled as a fluid continuum with the differential equations derived above and solved using the usual methods.

Runs presented in this paper use a 47-by-22 structured nonuniform grid encompassing the acceleration channel and approximately $4cm$ of the plume. Rotational symmetry is assumed. Therefore, only a meridional section of the Hall thruster acceleration zone is modeled. Grid spacing is determined by the timestep of the simulation. It is set not to exceed the maximum distance traveled by an ion particle in one timestep.

The magnetic field is generated as a pre-process by specifying the thruster geometry, assuming infinite permeability of the iron poles, and solving Laplace's equation on the regions exterior to the poles. The coils are assumed to be perfect solenoids, so the problem reduces to that of potential flow, with each pole piece set to a given magnetic potential.

The motion of heavy particles is slow compared to the electrons. For computational efficiency, the electrons and heavy particles are moved on different timesteps. Fig. 3 shows the sequence. Since T_e does not vary along magnetic field lines ($T_e = T_e(\lambda)$), it is possible to reduce the electron energy equation to a quasi-one-dimensional form. After some manipulation, a one-dimensional nonlinear differential equation is derived for T_e as a function of λ. The solution of this equation is accomplished by using a modified Forward Time Centered Space (FTCS) method.[15] The timestep

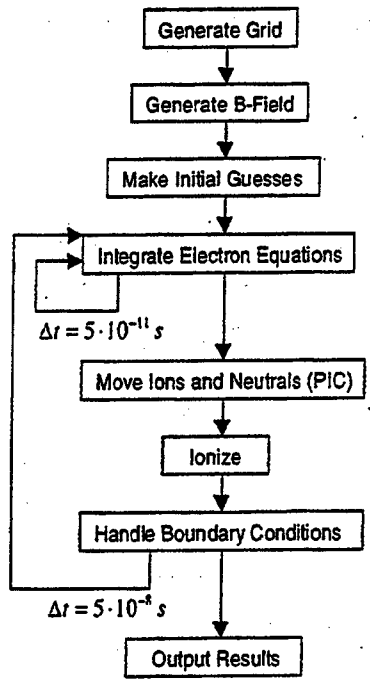

Fig. 3. Execution sequence of the numerical simulation.

is $5 \cdot 10^{-11}$ seconds, based on successive reduction to the case where the solution is stable and unchanging for smaller timesteps. Once T_e and ϕ^* are known on the domain, ϕ is found using Eqn. (1).

The electric field and electron temperature, determined by integrating the electron equations, is then used in a PIC method for ions and neutrals. Ion positions and velocities are updated. Also, the densities are adjusted appropriately based on computed local bulk ionization rate. This sequence repeats as shown in Fig. 3.

Since the method is time-accurate, the simulation will not, in general, converge to a steady state solution because of plasma fluctuations. Nevertheless, a solution is considered complete when the fluctuations reach a regular frequency and amplitude, and have repeated many periods. For this paper, results are averaged over $0.5ms$. One case takes approximately 5 hours to converge on a Pentium II Xeon–class personal computer.

Results and Discussion

Several cases were run to examine the effect of varying the secondary electron emission of the insulator wall. These cases are shown in Table 1 in order of decreasing secondary electron emission

Table 1. Performance results from the numerical simulation for various secondary electron emission coefficients of the wall material.

	Experiment	CASE 1	CASE 2	CASE 3	CASE 4	CASE 5
A	N/A	0.144	0.126	0.114	0.104	0.096
$T_{e,BP}(eV)$	N/A	16.0	20.0	24.0	28.0	32.0
$T_{e,max}(eV)$	N/A	15.5	19.03	22.2	25.0	27.4
$I_d(A)$	2.23	2.27	2.40	2.47	2.52	2.53
$I_b(A)$	1.61	1.45	1.53	1.58	1.60	1.61
$F(mN)$	37.8	37.2	39.3	40.5	41.1	41.4
η_u	0.938	0.844	0.891	0.920	0.932	0.938
η_d	0.722	0.639	0.638	0.640	0.635	0.636
η_c	0.673	0.805	0.806	0.803	0.806	0.810
η	0.456	0.434	0.458	0.473	0.477	0.483
F^{**}	N/A	0.052	0.064	0.074	0.080	0.086

coefficient, A, from (5). The exponential component, B, of the secondary electron emission model was constant at 0.576.

Geometry is that of an SPT-70. Operational parameters are $V_d = 300V$ and $\dot{m} = 2.34mg/s$. The first case in Table 1 is experimental, and was run at AFRL.[16] Some experimental values are marked "N/A" in Table 1 because they were not accurately measured. The remaining independent experimental measurands, I_d, I_b, and F have estimated accuracy of 2%, 10%, and 5%, respectively.[6]

The profile of electron temperature for Case 1 is shown in Fig. 4. The electric field is strongest near the exit of the channel. This causes Ohmic heating of the electrons in this region. Their energy decreases closer to the anode because of inelastic collision losses, and because of wall losses. The contours of electron temperature for Cases 2-5 are nearly identical to Case 1, except the magnitude increases with decreasing secondary electron emission coefficient. The peak temperature, $T_{e,max}$, always occurs at the exit, and is given for each case in Table 1.

The increase in T_e with decreasing secondary electron emission coefficient can be understood in the following way. Assuming wall interactions are the primary mechanism of electron energy loss, T_e can be expected to grow until limited by wall losses. As can be seen in Fig. 2, the heat flux to the walls increases rapidly as T_e approaches $T_{e,BP}$. Thus, $T_{e,BP}$ becomes the limit of electron temperature. Now, from (8) and (11), decreasing the secondary emission coefficient of the wall material increases $T_{e,BP}$, and, therefore, $T_{e,max}$.

Efficiencies shown in Table 1 are for the discharge only, excluding cathode flow. Breakdown of thrust efficiency may be given by[17] $\eta = \eta_u \eta_d \eta_c$, where:

$$\eta_u = \frac{I_b m_i}{e\dot{m}}$$
$$\eta_d = \frac{I_b}{I_d} \qquad (18)$$
$$\eta_c = \frac{V_b}{V_d}$$

Above, I_b is the ion beam current, I_d is the discharge

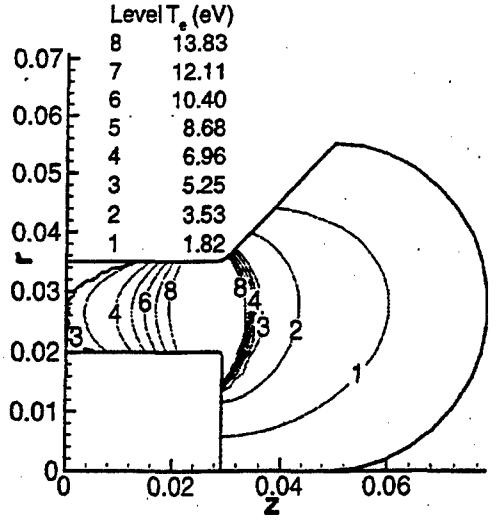

Fig. 4. Electron temperature contours in the SPT-70 discharge channel computed by *HPHall*. Case 1.

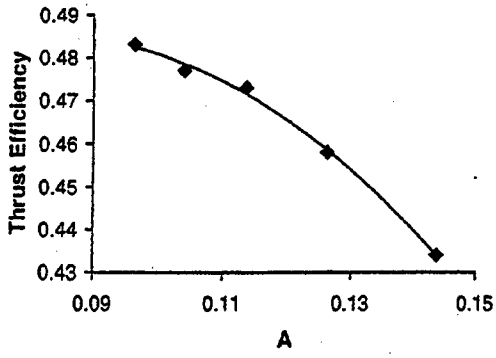

Fig. 5. Thrust efficiency versus secondary electron emission coefficient. For Cases 1-5.

current. V_i is the mean ion beam energy in Volts, and V_d is the discharge Voltage.

As secondary electron emission coefficient is decreased, electron temperature increases, as does the ionization efficiency of the plasma. This is reflected in the growth of utilization efficiency, η_u, with $T_{e,max}$ for Cases 1-5. Fig. 5 shows a plot of total efficiency versus secondary electron emission coefficient, A, for Cases 1-5. This is an important result, because it illuminates a predictable connection between secondary electron emission and thruster performance.

Another noticeable result shown in Table 1 is the increase in fraction of double ions in the beam, $F^{++} = I_{b,Xe^{++}} / I_{b,total}$, with decreasing secondary electron emission coefficient, A. This can be attributed to the cross section of double ionization by electron impact, which has a threshold just above 20 eV. The small changes in F^{++} observed here would have a negligible effect on thruster efficiency, but may be an important consideration for studying the interaction of Hall thruster beams with real spacecraft components.

Summary

As the secondary electron emission coefficient was decreased by two-thirds, *HPHall* predicted a steady increase in Hall thruster efficiency from 0.434 to 0.483. This indicates a relationship between secondary electron emission of Hall thruster insulator wall material and thruster performance. It suggests that secondary electron emission be one of the parameters considered during the Hall thruster design phase, and that materials with low secondary electron emission should be favored.

References

[1]Lentz, C. A., "Transient One Dimensional Numerical Simulation of Hall Thrusters", Massachusetts Institute of Technology, S.M. Thesis, 1993.

[2]Hirakawa, M., and Y. Arakawa, "Particle Simulation of Plasma Phenomena in Hall Thrusters," 24th International Electric Propulsion Conference, Moscow, Russia, 1995.

[3]Fife, J. M., and M. Martinez-Sanchez, "Two-Dimensional Hybrid Particle-In-Cell (PIC) Modeling of Hall Thrusters," 24th IEPC, Moscow, Russia, September 1995.

[4]Fife, John M., and Manuel Martinez-Sanchez, "Comparison of Results from a Two-Dimensional Numerical SPT Model with Experiment," 32nd AIAA/ASME/SAE/ASEE Joint Propulsion Conference, Lake Buena Vista, FL, 1996.

[5]Fife, J. M., Martinez-Sanchez, M., and Szabo, J., "A Numerical Study of Low-Frequency Discharge Oscillations in Hall Thrusters," 33rd AIAA/ASMA/SAE/ASEE Joint Propulsion Conference, Seattle, Washington, July 1997.

[6]Fife, J. M., Hybrid-PIC Modeling and Electrostatic Probe Survey of Hall Thrusters, Ph.D. Thesis, Massachusetts Institute of Technology, September 1998.

[7]Mitchner and Kruger, Partially Ionized Gasses, John Wiley & Sons, New York, 1973.

[8]Janes, G. S. and R. S. Lowder, "Anomalous Electron Diffusion and Ion Acceleration in a Low-Density Plasma," Physics of Fluids, 9, P. 1115, 1966.

[9]Bohm, D., Burhop, E.H.S., and Massey, H.S.W., in "Characteristics of Electrical Discharges in Magnetic Fields," A. Guthrie and R. K. Waterling, Eds., McGraw-Hill, New York, 1949.

[10]Dugan, John V. and Sovie, Ronald J., "Volume Ion Production Costs in Tenuous Plasmas: A General Atom Theory and Detailed Results for Helium, Argon and Cesium," NASA TN D-4150.

[11]Grishin, S. D., and L. V. Leskov, Electrical Rocket Engines of Space Vehicles, a partially-edited machine translation of Elektricheskikh Raketnyye Dvigateli Kosmicheskikh Apparatov, Publishing House "Mashinostroyeniye", Moscow, 1989, pp.1-216.

[12] Katz, I., et al, "The Importance of Accurate Secondary Electron Yields in Modeling Spacecraft Charging," Journal of Geophysical Research, V. 91, No. A12, December 1, 1986.

[13]Bugeat, J. P., Koppell, C., "Development of a Second Generation of SPT," 24th International Electric Propulsion Conference, Moscow, Russia, September 12-23, 1995.

[14]Fife, J. M. and M. Martinez-Sanchez, "Numerical Simulation of Facility Effects on Hall Thruster Performance," 26th International Electric Propulsion Conference, Kitakyushu, Japan, October 1999.

[15]Anderson. D. A.. Tannehill. J. C.. and Pletcher. R. H.. Computational Fluid Mechanics and Heat Transfer. Hemisphere Publishing Corporation. New York. 1984.

[16]Fife. J. M. and M. Martinez-Sanchez. "Characterization of the SPT-70 Plume Using Electrostatic Probes." 34th AIAA/ASMA-/SAE/ASEE Joint Propulsion Conference. Cleveland. Ohio. 1998.

[17]Komurasaki. K.. Hirakawa. M. and Y. Arakawa. "Plasma Acceleration Process in a Hall-Current Thruster". IEPC-91-078. 22nd International Electric Propulsion Conference. Viareggio. Italy. Oct. 1991.